Published in final edited form as:
Mol Cell. 2011 March 4; 41(5): 543–553. doi:10.1016/j.molcel.2011.02.006.

Stalled fork rescue via dormant replication origins in unchallenged S phase promotes proper chromosome segregation and tumor suppression

Tsuyoshi Kawabata[1,2], **Spencer W. Luebben**[1], **Satoru Yamaguchi**[1,2,5], **Ivar Ilves**[3], **Ilze Matise**[2,4,6], **Tavanna Buske**[1,7], **Michael R. Botchan**[3], and **Naoko Shima**[1,2,*]

[1] Department of Genetics, Cell Biology and Development, University of Minnesota

[2] Masonic Cancer Center, Minneapolis, MN 55455 USA

[3] Department of Molecular and Cell Biology, Division of Biochemistry and Molecular Biology, University of California, Berkeley, Berkeley, CA 94720 USA

[4] College of Veterinary Medicine, University of Minnesota, St. Paul, MN 55108 USA

Summary

Eukaryotic cells license far more origins than are actually used for DNA replication, thereby generating a large number of dormant origins. Accumulating evidence suggests that such origins play a role in chromosome stability and tumor suppression, though the underlying mechanism is largely unknown. Here, we show that a loss of dormant origins results in an increased number of stalled replication forks even in unchallenged S phase in primary mouse fibroblasts derived from embryos homozygous for the *Mcm4*^{Chaos3} allele. We found that this allele reduces the stability of the MCM2-7 complex, but confers normal helicase activity *in vitro*. Despite the activation of multiple fork recovery pathways, replication intermediates in these cells persist into M phase, increasing the number of abnormal anaphase cells with lagging chromosomes and/or acentric fragments. These findings suggest that dormant origins constitute a major pathway for stalled fork recovery, contributing to faithful chromosome segregation and tumor suppression.

Introduction

Replication origin licensing is a prerequisite for genome duplication, as DNA synthesis in S phase initiates exclusively from licensed origins (reviewed in Sclafani and Holzen, 2007). This process is restricted to the late M and early G1 phases, during which heterohexamers of the six minichromosome maintenance proteins (MCM2-7) are loaded onto origin recognition complex (ORC)-bound chromatin sites (reviewed in Forsburg, 2004; Tye, 1999). In the ensuing S phase, origins fire only once, when chromatin-bound MCM2-7 forms a replicative helicase complex (CMG complex) with cofactors CDC45 and GINS, unwinding the DNA (Ilves et al., 2010; Moyer et al., 2006). Active MCM2-7 complexes are then likely

*Corresponding author: shima023@umn.edu.
[5]General Surgical Science/Education and Research Support Center, Gunma University Graduate School of Medicine, 3-39-22 Showa-machi, Maebashi, Gunma, 371-8511, Japan
[6]Faculty of veterinary medicine, Latvia university of agriculture, K. Helmana str 8 Jelgava, LV-3004, Latvia.
[7]College of Pharmacy, Division of Pharmacology and Toxicology, University of Texas, Austin, Texas 78712-1010

to travel along with ongoing replication forks, returning fired origins to the unlicensed state (Todorov et al., 1995; Yan et al., 1993). Following S phase entry, multiple factors prohibit origin relicensing, thereby preventing rereplication of DNA (Blow and Dutta, 2005). It should be noted that the majority of replication origins in mammalian cells are not defined by specific DNA sequences (Gilbert, 2004).

It is known that an excessive amount of MCM2-7 complex are loaded onto respective ORC-bound chromatin sites (Bowers et al., 2004; Edwards et al., 2002) and that these complexes are presumably competent to initiate origin firing if permitted (Edwards et al., 2002; Ge et al., 2007; Ibarra et al., 2008). So, while a huge excess of potential origins exists throughout the genome in eukaryotic cells, only a fraction of them is apparently sufficient for DNA replication (Cortez et al., 2004; Woodward et al., 2006). Therefore, the role of such excess chromatin-bound MCM2-7 complexes has not been well understood.

Recent studies have investigated the role of these excess origins in human cancer cell lines (Ge et al., 2007; Ibarra et al., 2008). Consistent with an overabundance of MCM2-7 complexes on chromatin, up to 90% depletion of the MCM2-7 proteins had little effect on the densities of active origins in unperturbed S phase. However, MCM2-7 depleted cells did exhibit poor survival in the presence of low levels of the replication inhibitors aphidicolin (APH) or hydroxyurea. These findings suggest that dormant origins licensed by excess MCM2-7 complexes are most likely used as backups for “emergency” situations by increasing the number of replication forks, promoting the completion of DNA replication. However, it should be noted that the use of cancer cell lines in these studies might have hindered the ability to reveal the true role of dormant origins *in vivo*, as they exhibit greatly upregulated expression of the MCM2-7 proteins (Ha et al., 2004; Ishimi et al., 2003). Although it was previously thought that dormant origins are essentially dispensable in unperturbed S phase (Ge et al., 2007; Ibarra et al., 2008), we and others have reported that a reduced level of MCM2-7 proteins causes spontaneous tumors in mice with complete penetrance (Chuang et al., 2010; Kunnev et al., 2010; Pruitt et al., 2007; Shima et al., 2007), suggesting that dormant origins play an important role in such conditions. These mouse models exhibit a high level of spontaneous micronuclei in erythrocytes, a surrogate phenotype for chromosome instability (Pruitt et al., 2007; Shima et al., 2007). However, it remained to be determined whether chromosome instability occurs in other types of cells in these mice and how it is generated upon a loss of dormant origins, leading to spontaneous tumorigenesis in these mice.

Here, we used the *Mcm4*^{Chaos3} allele to investigate the complex role of dormant origins in chromosome stability, as the Phe345Ile change encoded by this allele compromises the stability of the MCM2-7 complex and leads to a reduced number of dormant origins. We found that this loss of dormant origins results in an accumulation of stalled replication forks in unchallenged S phase. Furthermore, despite the activation of multiple DNA repair pathways, a significant fraction of stalled forks persist into M phase and interfere with chromosome segregation.

Results

Chromatin-bound MCM2-7 protein levels are significantly reduced in *Mcm4*$^{Chaos3/Chaos3}$ MEFs, resulting in a loss of dormant origins

Previously, we reported that *Mcm4*^{Chaos3} homozygosity causes lower levels of the MCM2-7 proteins (Shima et al., 2007). As these proteins exist in vast excess of the number of replication origins that fire in S phase, we investigated whether *Mcm4*^{Chaos3} homozygosity also causes lower levels of chromatin-bound MCM2-7 proteins in primary fibroblasts (MEFs) isolated from *Mcm4*$^{Chaos3/Chaos3}$ embryos. Western blots (Figure 1A) revealed an

approximately 60% reduction of all components of the MCM2-7 complex on chromatin compared to wildtype cells. Chromatin immunoprecipitation followed by quantitative polymerase chain reaction also gave a similarly reduced rate of MCM2 at all specific loci examined (Figure S1A). To verify this reduced amount of dormant origins in *Mcm4*$^{Chaos3/Chaos3}$ cells, we performed a DNA fiber assay using consecutive dual labeling of two kinds of modified dUTPs (Sugimura et al., 2007) (Figure 1B). Previous studies (Ge et al., 2007; Ibarra et al., 2008; Kunnev et al., 2010) have demonstrated that a moderate loss of the MCM2-7 complexes from chromatin has little effect on active origin density in untreated conditions. Indeed, there was no difference in the average origin-to-origin distances between wildtype and *Mcm4*$^{Chaos3/Chaos3}$ MEFs in untreated conditions (49.1±2.6 kb and 49.6±3.8 kb, respectively; Figure 1C and Figure S1B). However, in the presence of APH, which triggers dormant origin firing (Ge et al., 2007), the average origin-to-origin distance in wildtype cells was reduced to 37.4±1.9 kb, significantly smaller than the 41.5±0.97 kb observed in *Mcm4*$^{Chaos3/Chaos3}$ cells (Figure 1C and Figure S1B). These findings collectively support the idea that *Mcm4*$^{Chaos3/Chaos3}$ cells have a significantly reduced number of dormant origins.

Mcm4$^{Chaos3/Chaos3}$ cells have an increased number of spontaneously stalled forks

Even in unchallenged conditions, we found that *Mcm4*$^{Chaos3/Chaos3}$ cells had nearly twice as many asymmetric bidirectional forks (one fork being stalled) as wildtype cells (Figure 1D). These observations suggest that fork stalling occurs at a higher frequency in *Mcm4*$^{Chaos3/Chaos3}$ cells and may explain why they show reduced levels of replication proteins on chromatin, such as proliferating cell nuclear antigen (PCNA) and CDC45 (Figure 1A). Indeed, we found that an increased number of *Mcm4*$^{Chaos3/Chaos3}$ cells were positive for discrete, bright RPA32 foci (Figure 2A), which form at stalled replication forks (Byun et al., 2005; Zou and Elledge, 2003). Moreover, the frequency of *Mcm4*$^{Chaos3/Chaos3}$ cells positive for RAD17 phosphorylated at Ser645 (pRAD17) (Bao et al., 2001) was increased about two-fold in untreated conditions (Figures 2A). RAD17 is a substrate of ATR and is involved in fork recovery (Bao et al., 2001). It functions upstream of CHK1, a major effector kinase in the ATR pathway (Wang et al., 2006). Previous studies reported that MCM depletion compromises checkpoint signaling in human cancer cell lines (Cortez et al., 2004; Tsao et al., 2004). However, *Mcm4*$^{Chaos3/Chaos3}$ cells exhibited levels of CHK1 phosphorylation at Ser345 (pCHK1) similar to wildtype when challenged (Figure S2), suggesting that there is no major defect in the ATR-CHK1 pathway. This observation is consistent with data from a recent study using *Mcm2* hypomorphic mouse cells (Kunnev et al., 2010). Despite relatively consistent detection of pRAD17 foci (Figure 2A), pCHK1 was barely detectable in unchallenged *Mcm4*$^{Chaos3/Chaos3}$ cells (Figure S2). This may indicate that the number of stalled forks in *Mcm4*$^{Chaos3/Chaos3}$ cells is still not sufficient to induce full activation of the ATR-CHK1 pathway, allowing cell cycle progression in the majority of *Mcm4*$^{Chaos3/Chaos3}$ cells. Stalled forks can potentially collapse, leading to the formation of double strand breaks (DSBs). *Mcm4*$^{Chaos3/Chaos3}$ cells exhibited only a modest increase in the formation of γH2AX foci, a marker of DSBs (Rogakou et al., 1998) in S phase (Figures 2B, left). It should be noted that only a small percentage of S phase cells were positive for γH2AX foci regardless of genotype (Figure 2B). Thus, stalled forks appear to be stably maintained during S phase.

The Phe345Ile change impairs the stability of the MCM2-7 complex, but not helicase activity

To understand what causes fork stalling in *Mcm4*$^{Chaos3/Chaos3}$ cells, we measured fork velocity using the DNA fiber technique (Figure 1B). Surprisingly, fork velocity was actually faster in *Mcm4*$^{Chaos3/Chaos3}$ cells compared to wildtype (Figure S1C). This apparently faster fork velocity could be partially explained by a lower level of fork terminations in

Mcm4$^{Chaos3/Chaos3}$ cells due to a loss of dormant origins (see Figures S1D and E). The helicase functions of the MCM2-7 complex are carried out in the CMG complex (Ilves et al., 2010; Costa et al., in press). As the phenylalanine residue mutated in *Mcm4*$^{Chaos3/Chaos3}$ cells lies in a highly conserved domain (Figure S3A), we reconstituted the *Drosophila* CMG complex with the same mutant MCM4 to investigate its actual helicase activity. The mutant complex was purified with a stoichiometry identical to wildtype (Figure 3A). Interestingly, the mutant CMG was slightly more efficient helicase than the wildtype CMG (Figure 3B), which may explain the faster fork speed in *Mcm4*$^{Chaos3/Chaos3}$ cells (Figures S1C-D). However, the lower yields of the mutant CMG complex prompted us to examine the stability of the mutant MCM2-7 complex. Wildtype and mutant MCM2-7 complexes were purified and subjected to analytical fractionation. While the wildtype complexes were stable, it was clear that the mutant complexes dissociated into sub-fractions (Figure 3C), reflecting a suspected weaker association between MCM6 and MCM4 (Figure S3B). Similarly reduced interactions between MCM6 and MCM4 were also found in *Mcm4*$^{Chaos3/Chaos3}$ cells (Figure S3C). Therefore, these weaker associations are the most likely cause of the instability of the mutant complex, thereby contributing to a decreased amount of MCM2-7 proteins. Taken together, these data suggest that a loss of dormant origins, rather than a defect in helicase activity, is the major cause of stalled fork accumulation in *Mcm4*$^{Chaos3/Chaos3}$ cells.

Mcm4$^{Chaos3/Chaos3}$ cells exhibit significantly elevated levels of RAD51 and BLM foci

Stalled forks can be rescued by homology-directed repair involving RAD51 (Petermann et al., 2010). We found that *Mcm4*$^{Chaos3/Chaos3}$ cells exhibit a mild increase (~2 fold) in spontaneous RAD51 foci formation (Figure 4A) and a drastic increase in foci formation for BLM helicase (Figure 4B), another protein involved in stalled fork recovery that counteracts RAD51 (Bugreev et al., 2007; Davies et al., 2007). As yeast *mcm* mutants exhibit a hyper-recombination phenotype (Gibson et al., 1990; Li et al., 2009), we measured the frequency of homologous recombination (HR) events using the *FYDR* (fluorescent yellow direct repeat) transgenic locus system (Figure S4A-B) (Hendricks et al., 2003). *Mcm4*$^{Chaos3/Chaos3}$ MEFs exhibited slightly higher frequencies of spontaneous HR events at this locus (Figure 4C and Figure S4C), but were not significantly different from wildtype. Next, we challenged these MEFs with APH, which induces fork stalling and RAD51 foci formation (Figure 4A). Unlike treatment with a higher dose of APH (3μM) or camptothecin (CPT), an inducer of DSBs at replication forks (Saleh-Gohari et al., 2005) (see Figure S2), a low dose of APH did not increase HR events (Figure 4D). Therefore, the rescue of stalled forks in *Mcm4*$^{Chaos3/Chaos3}$ cells may occur via the RAD51/BLM-mediated pathways without a significant increase in canonical HR events.

The occurrence of replication intermediates marked by FANCD2 sister foci in prophase is markedly enhanced in *Mcm4*$^{Chaos3/Chaos3}$ cells, leading to an increased level of micronucleus formation

Recent studies reported that unreplicated regions flanked by two stalled forks can persist into M phase and are marked with sister foci of FANCD2, a Fanconi anemia protein that presumably directs the resolution of such structures (Chan et al., 2009; Naim and Rosselli, 2009). To investigate whether stalled forks are resolved before M phase entry in *Mcm4*$^{Chaos3/Chaos3}$ cells, we examined the formation of FANCD2 sister foci in prophase. While FANCD2 sister foci were very rarely found in wildtype cells, nearly 50% of *Mcm4*$^{Chaos3/Chaos3}$ cells were positive for such foci at prophase (Figures 5A). Higher numbers of FANCD2 foci were also observed in *Mcm4*$^{Chaos3/Chaos3}$ cells throughout M phase (Figure S5A). We also found that foci formation for FANCI, a critical FANCD2 interacting-protein (Sims et al., 2007; Smogorzewska et al., 2007), was drastically increased in *Mcm4*$^{Chaos3/Chaos3}$ cells as well (Figure S5B). This drastic increase in FANCD2 sister foci was associated with an elevated incidence of aberrant anaphase cells containing lagging

and/or acentric chromosomes (Figure 5B). In accord with such structures in anaphase leading to micronucleus formation (Naim and Rosselli, 2009), *Mcm4*$^{Chaos3/Chaos3}$ cells also exhibited a 2-fold increase in spontaneous MN compared to wildtype cells (Figure 5B). This is a relatively small increase compared to the 20-fold increase observed in erythrocytes, the original phenotype that led to the identification of *Mcm4*^{Chaos3} (Shima et al., 2007). However, this can be attributed to the specific nature of erythrocytes as enucleated cells, as MN may occur more frequently in the absence of functional DNA repair and checkpoint responses in erythroblasts.

Mcm4$^{Chaos3/Chaos3}$ cells exhibit chromosome number and structural instability in late M phase

To understand the extent by which lagging chromosomes contribute to MN formation in *Mcm4*$^{Chaos3/Chaos3}$ cells, we quantitated the number of MN positive for the centromeric protein CENP-A (Howman et al., 2000). We found that the incidence of CENP-A positive MN is significantly elevated in *Mcm4*$^{Chaos3/Chaos3}$ cells compared to wildtype (Figure 5C), indicating an increased level of aneuploidy. Since aneuploid cells are rare and may have a reduced rate of proliferation (Williams et al., 2008), we performed interphase fluorescence in situ hybridization (FISH) using probes specific to near-centromeric regions of chromosome 16. This revealed not only a significant increase in aneuploidy in *Mcm4*$^{Chaos3/Chaos3}$ cells but also a significant increase in tetraploidy (Figure S5C). The exact mechanism responsible for tetraploidization has not been determined, but could result from cytokinesis failure (Movies S1-S3). Acentric chromosomes resulting from chromosome breaks, on the other hand, create CENP-A negative MN, which were found in ~40% of all MN in untreated *Mcm4*$^{Chaos3/Chaos3}$ cells (compare the MN frequencies in Figures 5B and 5C). As reported previously (Shima et al., 2007), G-banding analysis of metaphase chromosomes revealed no significant increase in spontaneous breaks in *Mcm4*$^{Chaos3/Chaos3}$ cells. However, it did reveal an increase in numerical and structural aberrations in *Mcm4*$^{Chaos3/Chaos3}$ cells, such as translocations and dicentric chromosomes (Figure 5D and S5D). Therefore, it is likely that acentric fragments arise after metaphase through the conversion of unresolved replication intermediates to DSBs. Indeed, we found a >2-fold increase in the number of MN positive for γH2AX foci in *Mcm4*$^{Chaos3/Chaos3}$ cells that had just completed mitosis (Figure 5E). Interestingly, we also found a significant increase in the number of γH2AX foci in the main nuclei of *Mcm4*$^{Chaos3/Chaos3}$ cells in early G1 phase (Figure S5E). These data indicate that unresolved replication intermediates are more susceptible to collapse after metaphase, giving rise to DSBs.

The chromosome instability seen in *Mcm4*$^{Chaos3/Chaos3}$ cells promotes the formation of a variety of spontaneous tumors

Previously, we reported that *Mcm4*$^{Chaos3/Chaos3}$ females in the C3HeB/FeJ (C3H) background develop mammary tumors only (Shima et al., 2007). Since tumor spectrum is strongly influenced by genetic background, as seen in *Mcm2* hypomorph mice (Kunnev et al., 2010), we bred *Mcm4*^{Chaos3} into the C57BL/6J (B6) strain to investigate the effect of genetic background on *Mcm4*^{Chaos3} tumorigenesis. All B6 *Mcm4*$^{Chaos3/Chaos3}$ females succumbed to neoplasms by the age of 16 months with a mean latency of 12.4 months (Figure 6A and Table S1). However, unlike C3H *Mcm4*$^{Chaos3/Chaos3}$ females, B6 *Mcm4*$^{Chaos3/Chaos3}$ females were highly prone to histiocytic sarcomas. Histiocytic sarcoma is a rare malignant proliferation of macrophage-like cells in humans and mice (Figure 6B) (Blackwell et al., 1995; Pileri et al., 2002). We also generated 21 F1 *Mcm4*$^{Chaos3/Chaos3}$ females by crossing B6 congenic (N8) and C3H congenic (N8) mice. All F1 *Mcm4*$^{Chaos3/Chaos3}$ females developed tumors with a mean latency of 14.2 months (Figure 6A and Table S2). Histiocytic sarcomas and lymphomas were the predominant neoplasms (Figures 6B and 6C) while three mammary adenocarcinomas were also observed. These data

suggest that the chromosome instability seen in *Mcm4*$^{Chaos3/Chaos3}$ cells (Figure 6D) is not restricted to mammary tumor formation but is relevant to the formation of a variety of tumors.

Discussion

In the present study, we used primary *Mcm4*$^{Chaos3/Chaos3}$ MEFs as a model to investigate the mechanism by which a loss of dormant origins confers chromosome instability. As summarized in Figure 6D, our findings suggest that a loss of dormant origins leads to the accumulation of stalled forks, ultimately resulting in incomplete DNA replication. The resulting unresolved replication intermediates are then carried over into M phase, thereby interfering with proper chromosome segregation. As a consequence, *Mcm4*$^{Chaos3/Chaos3}$ cells exhibit increased incidences of aneuploidy, chromosome breaks, translocations and tetraploidy, all of which are commonly observed in cancer cells. Given the high tumor predisposition of *Mcm4*$^{Chaos3/Chaos3}$ mice, the chromosome instability seen in *Mcm4*$^{Chaos3/Chaos3}$ cells is likely to promote tumorigenesis. Collectively, these findings suggest that dormant origins exist in abundance because of their critical role in fork recovery in unchallenged S phase, thereby promoting chromosome stability and tumor suppression.

Even in unchallenged S phase, replication forks stall due to the presence of endogenous DNA lesions. It is currently thought that stalled forks can be recovered by 1) homology-directed repair, 2) translesion synthesis (TLS) with error-prone DNA polymerases, or 3) passive replication from an adjacent origin (Paulsen and Cimprich, 2007). The use of dormant origins for stalled fork rescue can be viewed as an example of the last option, although this option originally implied rescue by adjacent major origins without any *de novo* firing. Our data show that the average density of active origins remains unchanged between wildtype and *Mcm4*$^{Chaos3/Chaos3}$ cells in unchallenged S phase (Figure 1C). This observation supports the previously held notion (Ge et al., 2007) that only dormant origins in the vicinity of stalled forks are allowed to fire and are therefore not likely to be detected as clearly as major origins by DNA fiber analysis (see model in Figure S6). Further studies are needed to elucidate the molecular mechanisms responsible for the use of dormant origins for stalled fork rescue.

Among the multiple pathways for stalled fork recovery, how an appropriate pathway is chosen for spontaneously stalled forks is largely unknown. An increased frequency of spontaneously stalled forks in *Mcm4*$^{Chaos3/Chaos3}$ cells led us to hypothesize that dormant origins play a more significant role in the recovery of spontaneously stalled forks than previously anticipated (Ge et al., 2007; Ibarra et al., 2008). In agreement with this hypothesis, a loss of dormant origins appears to activate homology-directed repair for the recovery of stalled forks (Figure 4A). Moreover, a recent study showed that MCM depletion in human primary lymphocytes leads to an increase in RAD51 foci formation (Orr et al., 2010). Unlike some yeast *mcm* mutants (Gibson et al., 1990; Li et al., 2009; Liang et al., 1999), *Mcm4*$^{Chaos3/Chaos3}$ cells exhibited no significant increase in canonical HR events when measured at the *FYDR* locus. This finding is consistent with recent data (Petermann et al., 2010) and can also be explained by the anti-recombinogenic role of BLM (Bugreev et al., 2007), which also forms an elevated number of foci in *Mcm4*$^{Chaos3/Chaos3}$ cells (Figure 4B). It should be noted that this reporter assay detects only unequal recombination events with tract lengths of more than a few hundred bases. Therefore, our data cannot exclude the possibility of an increase in gene conversion events with much shorter tract lengths.

Despite the activation of homology-directed repair, stalled forks do not seem to be fully rescued, as >50% of *Mcm4*$^{Chaos3/Chaos3}$ cells exhibit FANCD2/I foci in prophase (Figure 5A and Figure S5B), a marker of unresolved replication intermediates (Chan et al., 2009; Naim

and Rosselli, 2009). These observations suggest that dormant origins could be a preferred option for fork recovery over other pathways. This idea is quite feasible, considering the possible harmful consequences of homology-directed repair and TLS, such as genome rearrangements (Lee et al., 2007) and point mutations (Prakash et al., 2005), respectively. A recent study reported that MCM depletion in human primary lymphocytes causes hyper-activation of the non-homologous end-joining (NHEJ) pathway, resulting in an increase in the mis-repair of DSBs (Orr et al., 2010). Interestingly, we found that *Mcm4*$^{Chaos3/Chaos3}$ cells exhibited an increased incidence of translocations and dicentric chromosomes (Figure 5D and S5D). Based on our model (Figure 6D), chromosome breakage is likely to occur in late M phase. It is then possible that these broken chromosome ends are repaired by NHEJ in G1 phase, generating translocations. Taken together, it can be hypothesized that the preferential use of dormant origins for stalled fork rescue occurs to prevent a possible increase in mis-repair events resulting from hyper-activated DNA repair pathways.

In contrast to the commonly held idea that stalled forks eventually collapse, we found that spontaneously stalled forks are actually well preserved in S phase in primary mouse cells (Figure 2B). In fact, a fraction of stalled forks persisted into M phase, as evidenced by an increased number of FANCD2/I foci in prophase (Figures 5A and S5B). While the majority of these stalled forks are likely to be resolved by the downstream Fanconi pathway, a certain fraction of them remain unresolved, presumably physically interconnecting sister chromatids (Chan et al., 2009; Naim and Rosselli, 2009). Our study showed that a loss of dormant origins alone is capable of inducing such chromosome missegregation events without any exogenous replication inhibitor. The persistence of stalled forks in *Mcm4*$^{Chaos3/Chaos3}$ cells also partially activates the ATR pathway, as evidenced by a significant increase in pRAD17 foci formation (Figure 2A). This may explain why there exists a subtle but significant level of *Mcm4*$^{Chaos3/Chaos3}$ cells accumulated at the G2/M phases as described previously (Shima et al., 2007). It should also be noted that a low level of unresolved replication intermediates apparently escape from any known cell cycle checkpoint, as previously demonstrated (Casper et al., 2002; Chan and Hickson, 2009).

Consistent with the role of dormant origins in tumor suppression, a recent study reported that tumor formation in *Mcm4*$^{Chaos3/Chaos3}$ mice is significantly delayed by increasing the levels of chromatin-bound MCM2-7 proteins (Chuang et al., 2010). We find that *Mcm4*$^{Chaos3/Chaos3}$ mice exhibit phenotypes very similar to what has been seen in *Mcm2* hypomorph mice (Kunnev et al., 2010; Pruitt et al., 2007), such as a modest increase in the levels of γH2AX and phosphorylated p53 (Figure S2). While it remains to be determined, *Mcm4*^{Chaos3} and *Mcm2* hypomorph mice may share essentially the same mechanism for tumorigensis. One striking difference between these two mouse models is tumor latency; *Mcm2* hypomorph mice develop tumors much faster than *Mcm4*$^{Chaos3/Chaos3}$ mice. As discussed elsewhere (Pruitt et al., 2007), this difference could be attributed to the distinct roles of each component of the MCM2-7 complex. Moreover, the presence of the transgene in *Mcm2* hypomorph mice may additionally contribute to tumorigenesis by altering the expression of nearby genes.

Chromosome instability is a hallmark of cancer cells. However, how it is generated is still not well understood. We found that an increased frequency of stalled forks is sufficient to induce multiple types of chromosome instability. This idea is also consistent with an emerging hypothesis that replication stress is the major cause of the chromosome instability observed in cancer (Halazonetis et al., 2008; Negrini et al., 2010). Since the majority of cancer-initiating events deregulate the proper G1/S transition (Sherr, 2000), a loss of dormant origins may occur at an early stage of carcinogenesis. In this context, the findings presented in this study are highly relevant to our understanding of cancer development.

Experimental Procedures

Animals and MEFs

Mcm4^{Chaos3} was introduced into the C57BL/6J (B6) and C3HeB/FeJ (C3H) backgrounds by backcrossing 7 times (N8). F1 mice were generated by crossing congenic B6 and C3H lines. All experiments involving mice were approved by the Institutional Animal Care and Use Committee (IACUC). MEFs were generated from 12.5–14.5 dpc embryos and cultured using a standard procedure. F1 MEFs were used for all experiments unless otherwise noted.

Western blotting and immunofluorescence microscopy

Western blotting and immunofluorescence staining were carried out using standard procedures. Cell fractionation was performed using the Qproteome Nuclear Protein Kit (Qiagen). Detailed procedures are provided in supplemental experimental procedures.

DNA fiber

We used the DNA fiber protocol previously developed by Sugimura et al (Sugimura et al., 2007). Briefly, ongoing forks were labeled with digoxigenin-dUTPs for 20 min and then with biotin-dUTPs for 30 min. Labeled cells were dropped onto slides, fixed and dipped into lysis buffer. The resulting DNA fibers were released and extended by tilting the slides. Incorporated dUTPs were then visualized by immunofluorescent detection using anti digoxigenin-Rhodamine (Roche) and streptavidin-Alexa-Fluor-488 (Invitrogen).

HR events at the FYDR locus

HR-positive recombinant cells were detected by methods described previously (Hendricks et al., 2003). Detailed procedures are provided in supplemental experimental procedures.

Aberrant anaphase and cytokinesis-block micronucleus assays

For both analyses, cells were cultured on cover slips, fixed and stained with DAPI for fluorescence microscopy. At least 100 anaphases were scored per experiment. To score micronuclei, cytochalasin B (0.72 μg/ml) was added to block cytokinesis 16 hours before harvest. The resulting binucleated cells were scored for the presence of micronuclei. At least 200 binucleated cells were scored per experiment. For the CENP-A and γH2AX analyses, cells were subjected to antibody treatment following fixation.

Purification and characterization of the MCM2-7 and CMG complexes

The baculovirus vector expressing the *Drosophila melanogaster* MCM4^{Chaos3} protein was constructed by standard PCR-based site directed mutagenesis and the Invitrogen Bac-to-Bac protocol. The conserved residue Phe349 was replaced by Ile in the resulting mutant protein. The purification of the *Drosophila* CMG and MCM2-7 complexes was performed as described previously (Ilves et al., 2010). The MCM3 and Sld5 proteins carry N-terminal flag and HA affinity tags, respectively. For the MCM2-7 stability experiments, fractions from the Mono Q HR 5/5 column chromatography step that contained the MCM 2-7 hexameric complex were pooled and injected onto the Mono Q PC 1.6/5 column connected to the Pharmacia SMART micro purification system. The column was developed with 10 column volumes of linear 300-1100 mM potassium acetate gradient, and 20 fractions were collected and analysed by SDS-PAGE and coomassie brilliant blue staining. The DNA helicase assays were carried out with an M13-based circular substrate as described previously (Ilves et al., 2010), except that the ATP concentration was kept at 10 mM.

Supplementary Material

Refer to Web version on PubMed Central for supplementary material.

Acknowledgments

We thank Dr. Kazuto Sugimura for the DNA fiber protocol, Dr. Bevin Engelward for the FYDR mice as well as Drs. David Largaespada, Anja Bielinsky, and Alexandra Sobeck for their critical reading of the manuscript. We also thank Ms. LeAnn Oseth and Dr. B. Hirsch for the G-banding analyses and interpretations as well as Mr. Andy Lane for his assistance in the live-cell imaging experiments. This study was supported by grants (to N.S.) from Susan G Komen for the Cure (BCTR0707864) and the NCI (R01CA148806). The work at UC Berkeley was supported by the NIH grants CA R37-30490 (to M.R.B.).

References

Bao S, Tibbetts RS, Brumbaugh KM, Fang Y, Richardson DA, Ali A, Chen SM, Abraham RT, Wang XF. ATR/ATM-mediated phosphorylation of human Rad17 is required for genotoxic stress responses. Nature. 2001; 411:969–974. [PubMed: 11418864]

Blackwell BN, Bucci TJ, Hart RW, Turturro A. Longevity, body weight, and neoplasia in ad libitum-fed and diet-restricted C57BL6 mice fed NIH-31 open formula diet. Toxicol Pathol. 1995; 23:570–582. [PubMed: 8578100]

Blow JJ, Dutta A. Preventing re-replication of chromosomal DNA. Nat Rev Mol Cell Biol. 2005; 6:476–486. [PubMed: 15928711]

Bowers JL, Randell JC, Chen S, Bell SP. ATP hydrolysis by ORC catalyzes reiterative Mcm2-7 assembly at a defined origin of replication. Mol Cell. 2004; 16:967–978. [PubMed: 15610739]

Bugreev DV, Yu X, Egelman EH, Mazin AV. Novel pro- and anti-recombination activities of the Bloom's syndrome helicase. Genes Dev. 2007; 21:3085–3094. [PubMed: 18003860]

Byun TS, Pacek M, Yee MC, Walter JC, Cimprich KA. Functional uncoupling of MCM helicase and DNA polymerase activities activates the ATR-dependent checkpoint. Genes Dev. 2005; 19:1040–1052. [PubMed: 15833913]

Casper AM, Nghiem P, Arlt MF, Glover TW. ATR regulates fragile site stability. Cell. 2002; 111:779–789. [PubMed: 12526805]

Chan KL, Hickson ID. On the origins of ultra-fine anaphase bridges. Cell Cycle. 2009; 8:3065–3066. [PubMed: 19755843]

Chan KL, Palmai-Pallag T, Ying S, Hickson ID. Replication stress induces sister-chromatid bridging at fragile site loci in mitosis. Nat Cell Biol. 2009; 11:753–760. [PubMed: 19465922]

Chuang CH, Wallace MD, Abratte C, Southard T, Schimenti JC. Incremental Genetic Perturbations to MCM2-7 Expression and Subcellular Distribution Reveal Exquisite Sensitivity of Mice to DNA Replication Stress. PLoS Genet. 2010; 6:e1001110. [PubMed: 20838603]

Costa A, Ilves I, Tamberg N, Petojevic T, Nogales E, Botchan MR, Berger JM. The structural basis for MCM2-7 helicase activation by GINS and Cdc45. Nat Struct Mol Biol. in press.

Cortez D, Glick G, Elledge SJ. Minichromosome maintenance proteins are direct targets of the ATM and ATR checkpoint kinases. Proc Natl Acad Sci U S A. 2004; 101:10078–10083. [PubMed: 15210935]

Davies SL, North PS, Hickson ID. Role for BLM in replication-fork restart and suppression of origin firing after replicative stress. Nat Struct Mol Biol. 2007; 14:677–679. [PubMed: 17603497]

Edwards MC, Tutter AV, Cvetic C, Gilbert CH, Prokhorova TA, Walter JC. MCM2-7 complexes bind chromatin in a distributed pattern surrounding the origin recognition complex in Xenopus egg extracts. J Biol Chem. 2002; 277:33049–33057. [PubMed: 12087101]

Fenech M. Cytokinesis-block micronucleus cytome assay. Nat Protoc. 2007; 2:1084–1104. [PubMed: 17546000]

Forsburg SL. Eukaryotic MCM proteins: beyond replication initiation. Microbiol Mol Biol Rev. 2004; 68:109–131. [PubMed: 15007098]

Ge XQ, Jackson DA, Blow JJ. Dormant origins licensed by excess Mcm2-7 are required for human cells to survive replicative stress. Genes Dev. 2007; 21:3331–3341. [PubMed: 18079179]

Gibson SI, Surosky RT, Tye BK. The phenotype of the minichromosome maintenance mutant mcm3 is characteristic of mutants defective in DNA replication. Mol Cell Biol. 1990; 10:5707–5720. [PubMed: 2233713]

Gilbert DM. In search of the holy replicator. Nat Rev Mol Cell Biol. 2004; 5:848–855. [PubMed: 15459665]

Ha SA, Shin SM, Namkoong H, Lee H, Cho GW, Hur SY, Kim TE, Kim JW. Cancer-associated expression of minichromosome maintenance 3 gene in several human cancers and its involvement in tumorigenesis. Clin Cancer Res. 2004; 10:8386–8395. [PubMed: 15623617]

Halazonetis TD, Gorgoulis VG, Bartek J. An oncogene-induced DNA damage model for cancer development. Science. 2008; 319:1352–1355. [PubMed: 18323444]

Hendricks CA, Almeida KH, Stitt MS, Jonnalagadda VS, Rugo RE, Kerrison GF, Engelward BP. Spontaneous mitotic homologous recombination at an enhanced yellow fluorescent protein (EYFP) cDNA direct repeat in transgenic mice. Proc Natl Acad Sci U S A. 2003; 100:6325–6330. [PubMed: 12750464]

Howman EV, Fowler KJ, Newson AJ, Redward S, MacDonald AC, Kalitsis P, Choo KH. Early disruption of centromeric chromatin organization in centromere protein A (Cenpa) null mice. Proc Natl Acad Sci U S A. 2000; 97:1148–1153. [PubMed: 10655499]

Ibarra A, Schwob E, Mendez J. Excess MCM proteins protect human cells from replicative stress by licensing backup origins of replication. Proc Natl Acad Sci U S A. 2008; 105:8956–8961. [PubMed: 18579778]

Ilves I, Petojevic T, Pesavento JJ, Botchan MR. Activation of the MCM2-7 Helicase by Association with Cdc45 and GINS Proteins. Mol Cell. 2010; 37:247–258. [PubMed: 20122406]

Ishimi Y, Okayasu I, Kato C, Kwon HJ, Kimura H, Yamada K, Song SY. Enhanced expression of Mcm proteins in cancer cells derived from uterine cervix. Eur J Biochem. 2003; 270:1089–1101. [PubMed: 12631269]

Kunnev D, Rusiniak ME, Kudla A, Freeland A, Cady GK, Pruitt SC. DNA damage response and tumorigenesis in Mcm2-deficient mice. Oncogene. 2010; 29:3630–3638. [PubMed: 20440269]

Lee JA, Carvalho CM, Lupski JR. A DNA replication mechanism for generating nonrecurrent rearrangements associated with genomic disorders. Cell. 2007; 131:1235–1247. [PubMed: 18160035]

Li XC, Schimenti JC, Tye BK. Aneuploidy and improved growth are coincident but not causal in a yeast cancer model. PLoS Biol. 2009; 7:e1000161. [PubMed: 19636358]

Liang DT, Hodson JA, Forsburg SL. Reduced dosage of a single fission yeast MCM protein causes genetic instability and S phase delay. J Cell Sci. 1999; 112(Pt 4):559–567. [PubMed: 9914167]

Moyer SE, Lewis PW, Botchan MR. Isolation of the Cdc45/Mcm2-7/GINS (CMG) complex, a candidate for the eukaryotic DNA replication fork helicase. Proc Natl Acad Sci U S A. 2006; 103:10236–10241. [PubMed: 16798881]

Naim V, Rosselli F. The FANC pathway and BLM collaborate during mitosis to prevent micro-nucleation and chromosome abnormalities. Nat Cell Biol. 2009; 11:761–768. [PubMed: 19465921]

Negrini S, Gorgoulis VG, Halazonetis TD. Genomic instability--an evolving hallmark of cancer. Nat Rev Mol Cell Biol. 2010; 11:220–228. [PubMed: 20177397]

Orr SJ, Gaymes T, Ladon D, Chronis C, Czepulkowski B, Wang R, Mufti GJ, Marcotte EM, Thomas NS. Reducing MCM levels in human primary T cells during the G(0)-->G(1) transition causes genomic instability during the first cell cycle. Oncogene. 2010; 29:3803–3814. [PubMed: 20440261]

Paulsen RD, Cimprich KA. The ATR pathway: fine-tuning the fork. DNA Repair (Amst). 2007; 6:953–966. [PubMed: 17531546]

Petermann E, Orta ML, Issaeva N, Schultz N, Helleday T. Hydroxyurea-stalled replication forks become progressively inactivated and require two different RAD51-mediated pathways for restart and repair. Mol Cell. 2010; 37:492–502. [PubMed: 20188668]

Pileri SA, Grogan TM, Harris NL, Banks P, Campo E, Chan JK, Favera RD, Delsol G, De Wolf-Peeters C, Falini B, et al. Tumours of histiocytes and accessory dendritic cells: an

immunohistochemical approach to classification from the International Lymphoma Study Group based on 61 cases. Histopathology. 2002; 41:1–29. [PubMed: 12121233]

Prakash S, Johnson RE, Prakash L. Eukaryotic translesion synthesis DNA polymerases: specificity of structure and function. Annu Rev Biochem. 2005; 74:317–353. [PubMed: 15952890]

Pruitt SC, Bailey KJ, Freeland A. Reduced Mcm2 Expression Results in Severe Stem/Progenitor Cell Deficiency and Cancer. Stem Cells. 2007; 25:3121–3121. [PubMed: 17717065]

Rogakou EP, Pilch DR, Orr AH, Ivanova VS, Bonner WM. DNA double-stranded breaks induce histone H2AX phosphorylation on serine 139. J Biol Chem. 1998; 273:5858–5868. [PubMed: 9488723]

Saleh-Gohari N, Bryant HE, Schultz N, Parker KM, Cassel TN, Helleday T. Spontaneous homologous recombination is induced by collapsed replication forks that are caused by endogenous DNA single-strand breaks. Mol Cell Biol. 2005; 25:7158–7169. [PubMed: 16055725]

Sclafani RA, Holzen TM. Cell cycle regulation of DNA replication. Annu Rev Genet. 2007; 41:237–280. [PubMed: 17630848]

Sherr CJ. The Pezcoller lecture: cancer cell cycles revisited. Cancer Res. 2000; 60:3689–3695. [PubMed: 10919634]

Shi Q, King RW. Chromosome nondisjunction yields tetraploid rather than aneuploid cells in human cell lines. Nature. 2005; 437:1038–1042. [PubMed: 16222248]

Shima N, Alcaraz A, Liachko I, Buske TR, Andrews CA, Munroe RJ, Hartford SA, Tye BK, Schimenti JC. A viable allele of Mcm4 causes chromosome instability and mammary adenocarcinomas in mice. Nat Genet. 2007; 39:93–98. [PubMed: 17143284]

Sims AE, Spiteri E, Sims RJ 3rd, Arita AG, Lach FP, Landers T, Wurm M, Freund M, Neveling K, Hanenberg H, et al. FANCI is a second monoubiquitinated member of the Fanconi anemia pathway. Nat Struct Mol Biol. 2007; 14:564–567. [PubMed: 17460694]

Smogorzewska A, Matsuoka S, Vinciguerra P, McDonald ER 3rd, Hurov KE, Luo J, Ballif BA, Gygi SP, Hofmann K, D'Andrea AD, Elledge SJ. Identification of the FANCI protein, a monoubiquitinated FANCD2 paralog required for DNA repair. Cell. 2007; 129:289–301. [PubMed: 17412408]

Sugimura K, Takebayashi S, Ogata S, Taguchi H, Okumura K. Non-denaturing fluorescence in situ hybridization to find replication origins in a specific genome region on the DNA fiber. Biosci Biotechnol Biochem. 2007; 71:627–632. [PubMed: 17284819]

Todorov IT, Attaran A, Kearsey SE. BM28, a human member of the MCM2-3–5 family, is displaced from chromatin during DNA replication. J Cell Biol. 1995; 129:1433–1445. [PubMed: 7790346]

Tsao CC, Geisen C, Abraham RT. Interaction between human MCM7 and Rad17 proteins is required for replication checkpoint signaling. Embo J. 2004; 23:4660–4669. [PubMed: 15538388]

Tye BK. MCM proteins in DNA replication. Annu Rev Biochem. 1999; 68:649–686. [PubMed: 10872463]

Wang X, Zou L, Lu T, Bao S, Hurov KE, Hittelman WN, Elledge SJ, Li L. Rad17 phosphorylation is required for claspin recruitment and Chk1 activation in response to replication stress. Mol Cell. 2006; 23:331–341. [PubMed: 16885023]

Williams BR, Prabhu VR, Hunter KE, Glazier CM, Whittaker CA, Housman DE, Amon A. Aneuploidy affects proliferation and spontaneous immortalization in mammalian cells. Science. 2008; 322:703–709. [PubMed: 18974345]

Woodward AM, Gohler T, Luciani MG, Oehlmann M, Ge X, Gartner A, Jackson DA, Blow JJ. Excess Mcm2-7 license dormant origins of replication that can be used under conditions of replicative stress. J Cell Biol. 2006; 173:673–683. [PubMed: 16754955]

Yan H, Merchant AM, Tye BK. Cell cycle-regulated nuclear localization of MCM2 and MCM3, which are required for the initiation of DNA synthesis at chromosomal replication origins in yeast. Genes Dev. 1993; 7:2149–2160. [PubMed: 8224843]

Zou L, Elledge SJ. Sensing DNA damage through ATRIP recognition of RPA-ssDNA complexes. Science. 2003; 300:1542–1548. [PubMed: 12791985]

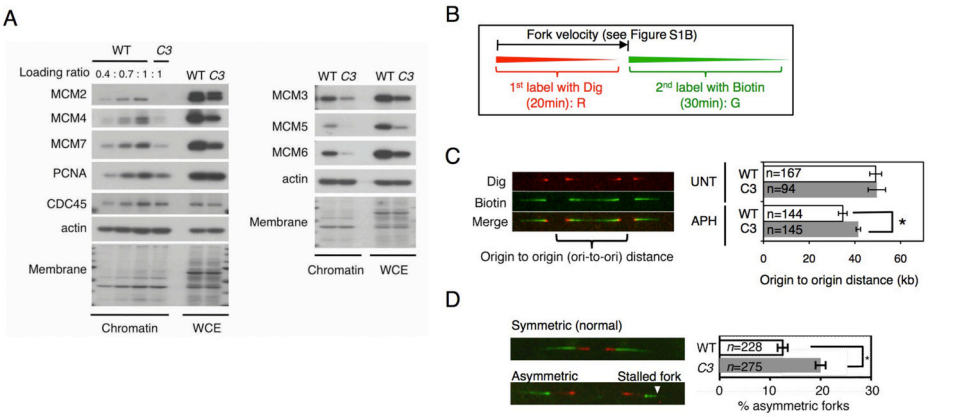

Figure 1. *Mcm4*$^{Chaos3/Chaos3}$ cells have reduced amounts of the MCM2-7 proteins on chromatin, resulting in a reduced number of dormant origins

(A) All components of the MCM2-7 complex are significantly reduced in *Mcm4*$^{Chaos3/Chaos3}$ cells. Reduction levels of chromatin-bound MCM2/4/7 as well as other replication proteins in *Mcm4*$^{Chaos3/Chaos3}$ (*C3*) cells were estimated by referencing wildtype (WT) proteins loaded in different amounts (left). In *Mcm4*$^{Chaos3/Chaos3}$ cells, the MCM3/5/6 proteins were also reduced in both the chromatin fraction and whole cell extract (WCE) (right). Protein samples were obtained from cells cultured asynchronously. Actin and stained membranes were used as loading controls.

(B) Schematic presentation of consecutive dual labeling in the DNA fiber assay. Replication forks were labeled with digoxigenin-dUTPs (dig-dUTPs, red) for 20 min followed by biotin-dUTPs (green) for 30 min.

(C) There is no significant difference in the average density of active origins between wildtype and *Mcm4*$^{Chaos3/Chaos3}$ cells in untreated conditions (UNT). However, APH treatment induced a significantly lower origin density in *Mcm4*$^{Chaos3/Chaos3}$ cells ($p<0.05$, t-test). These values were determined by measuring the distances between adjacent origins as shown (left). Bars show standard error of the mean (SEM).

(D) *Mcm4*$^{Chaos3/Chaos3}$ cells show a significant increase in the frequency of asymmetric forks (see image on the left). The average frequencies are shown with SEMs and are compared by χ2-test ($p<0.005$, see asterisk).

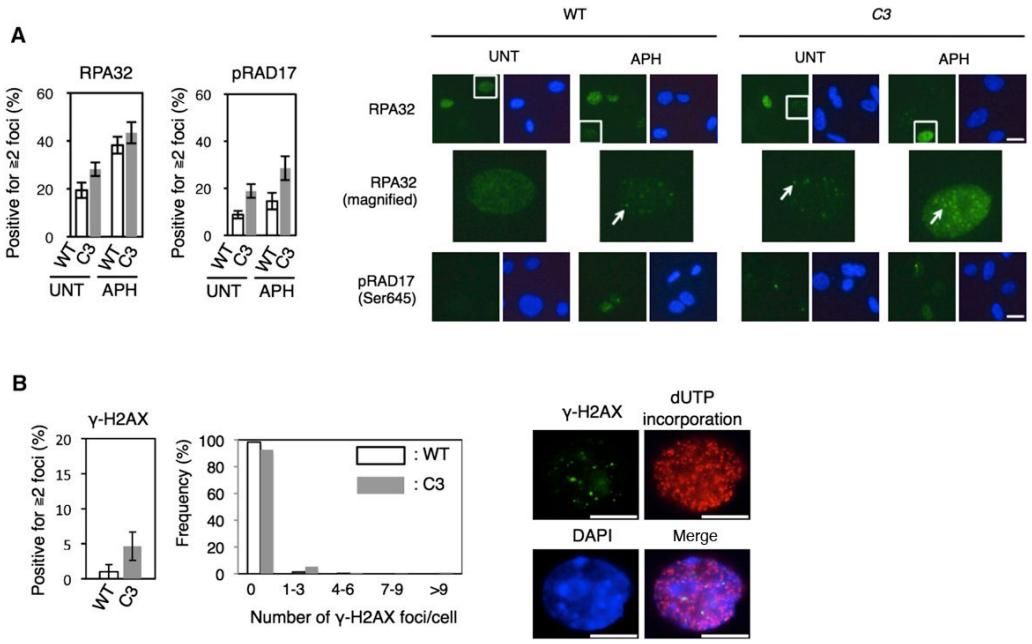

Figure 2. Elevated levels of RPA, pRAD17 and γH2AX foci formation are observed in *Mcm4*$^{Chaos3/Chaos3}$ cells

(A) An increased number of *Mcm4*$^{Chaos3/Chaos3}$ cells are positive for RPA32 and pRAD17 (Ser645) foci. Shown are the average percentages of cells positive for each marker in the untreated (UNT) and APH (300nM for 24 hrs) treated conditions. Bars are SEMs for ten different fields obtained from two independently performed experiments. Representative images are shown on the right with a magnified view of the selected nuclei. Nuclei are stained with DAPI (blue). Scale bars are 40 μm.

(B) *Mcm4*$^{Chaos3/Chaos3}$ cells show a slight increase in the formation of γH2AX foci in S phase. Shown are the average percentages of cells positive for γH2AX foci and the distribution of the number of γH2AX foci per cell in the untreated condition (left). S phase cells were detected by incorporation of dUTPs. Bars are SEMs for three independent experiments. Representative images are shown on the right. Scale bars are 10 μm.

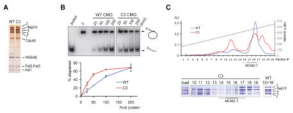

Figure 3. The mutant MCM2-7 complex is unstable but retains proper helicase activity in the CMG complex

(A) Silver stained 10% SDS-polyacrylamide gels (PAGE) show purified wildtype and mutant CMG complexes.

(B) An autoradiograph of a helicase assay showing the radiolabeled products separated by PAGE (top). M13 circular DNA annealed with a radiolabeled oligonucleotide was used as a substrate. The migration of double stranded substrate and displaced oligo is shown with arrows. The amount of protein in femtomoles in each reaction is indicated. The first two lanes show the completely denatured substrate and the substrate with no protein. The reactions were performed in duplicate and quantified as a percentage of substrate processed as shown in the bottom graph. Error bars show standard deviations.

(C) The salt elution profiles of wildtype and mutant MCM2-7 from Mono Q anion exchange chromatography show the relative instability of the mutant complex (top). Blue and red lines show the relative absorbance at 280 nm for the wildtype and mutant gradient runs, respectively (left Y axis); the grey axis indicates salt concentration (right Y axis). The peak protein fractions from the mutant gradient were separated by SDS-PAGE and stained with coomassie brilliant blue (bottom); the fraction numbers are shown above each lane. The starting stoichometric mutant MCM2-7 complex that was loaded onto this column is shown in the first lane and the pooled peak fractions (15 and 16) from the WT gradient are shown in the last lane.

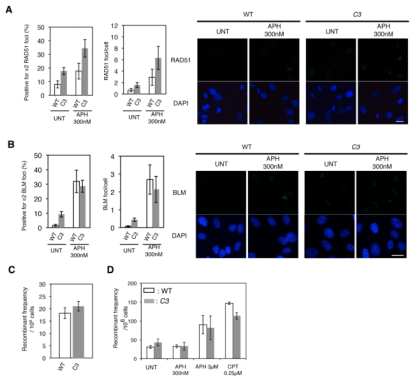

Figure 4. An increase in RAD51 and BLM foci formation in *Mcm4*$^{Chaos3/Chaos3}$ cells does not lead to a significant increase in homologous recombination events

(A) An increased number of *Mcm4*$^{Chaos3/Chaos3}$ cells are positive for RAD51 foci.

(B) BLM foci formation is drastically elevated in *Mcm4*$^{Chaos3/Chaos3}$ cells. Shown in A and B are the average percentages of cells positive for ≥2 foci in the untreated and APH treated conditions (left). The average number of foci per cell is also shown. Bars are SEMs for ten different fields obtained from two independently performed experiments. Representative images are shown on the right. Scale bars are 20 μm.

(C) No significant increase in HR events was detected at the *FYDR* locus in *Mcm4*$^{Chaos3/Chaos3}$ cells compared to wildtype. Bars are SEMs for recombinant frequencies determined by analyzing at least 16 embryos per genotype.

(D) No significant increase in HR events was detected at the *FYDR* locus in either wildtype or *Mcm4*$^{Chaos3/Chaos3}$ cells after a low dose of APH treatment. CPT and a higher dose of APH were used as positive controls. Bars are SEMs for recombinant frequencies determined by analyzing at least 3 independent MEF lines.

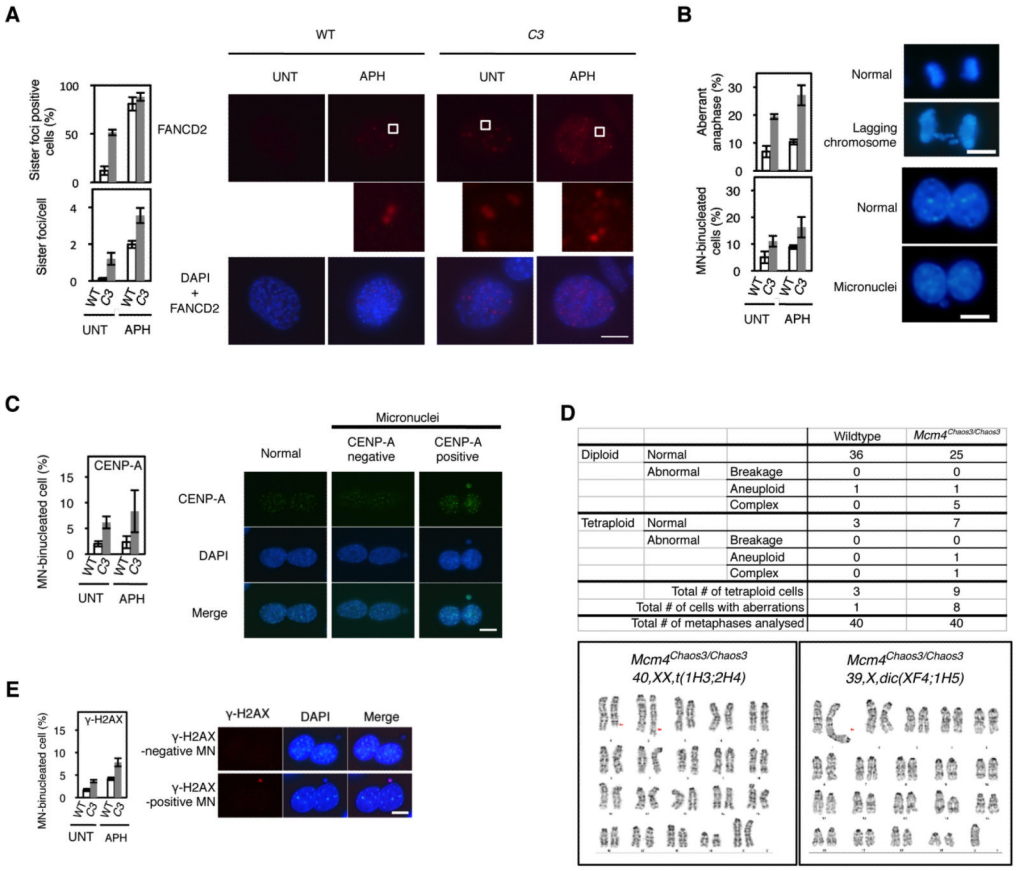

			Wildtype	$Mcm4^{Chaos3/Chaos3}$
Diploid	Normal		36	25
	Abnormal	Breakage	0	0
		Aneuploid	1	1
		Complex	0	5
Tetraploid	Normal		3	7
	Abnormal	Breakage	0	0
		Aneuploid	0	1
		Complex	0	1
	Total # of tetraploid cells		3	9
	Total # of cells with aberrations		1	8
	Total # of metaphases analysed		40	40

Figure 5. *Mcm4*$^{Chaos3/Chaos3}$ cells have a drastically increased number of FANCD2 sister foci at prophase, preceding abnormal anaphase and micronucleation

(A) An increased frequency of FANCD2 sister foci is found in *Mcm4*$^{Chaos3/Chaos3}$ cells. The average percentages of cells positive for FANCD2 sister foci (top) and the average numbers of FANCD2 sister foci per cell (bottom) are shown with SEMs. Note that the number of FANCD2 sister foci per cell increases approximately 2-fold in *Mcm4*$^{Chaos3/Chaos3}$ cells compared to wildtype cells, while nearly all cells become positive for such foci in the presence of APH. Representative images are shown on the right with a magnified view (indicated by squares).

(B) An increased number of *Mcm4*$^{Chaos3/Chaos3}$ cells undergo abnormal anaphase, forming micronuclei (MN). The average frequencies of abnormal anaphases containing lagging chromosomes and/or fragments are shown for wildtype and *Mcm4*$^{Chaos3/Chaos3}$ cells with SEMs (left, top). B6 MEFs were used for anaphase analysis. The average MN frequencies are also shown for wildtype and *Mcm4*$^{Chaos3/Chaos3}$ cells with SEMs (left, bottom). MN were detected using the cytokinesis-block micronucleus assay (Fenech, 2007). Representative images are shown on the right for a normal anaphase, an abnormal anaphase containing lagging chromosomes, a normal binucleated cell and one with a micronucleus. Scale bars are 5 μm.

(C) *Mcm4*$^{Chaos3/Chaos3}$ cells have an increased number of centromeric (CENP-A^{+}) MN compared to wildtype cells. The average frequencies of CENP-A^{+} MN were determined from three independently performed experiments and are shown with SEMs. Representative images are shown on the right.

(D) G-banding analysis of metaphase chromosomes shows no evidence for increased chromosome breaks but does reveal an increased occurrence of translocations in

Mcm4$^{Chaos3/Chaos3}$ cells. Representative karyotypes containing translocations are also shown bottom.

(E) *Mcm4*$^{Chaos3/Chaos3}$ cells have an increased number of γH2AX-foci-positive (γH2AX^{+}) MN compared to wildtype cells. The average frequencies of γH2AX $^{+}$ MN were determined from three independently performed experiments and are shown with SEMs. Representative images are shown on the right for MN positive and negative for γH2AX (red) in binucleated cells. APH was used as a positive control (150 nM for 24 hrs). Nuclei are stained with DAPI (blue). Scale bars (A, C and E) are 10 μm.

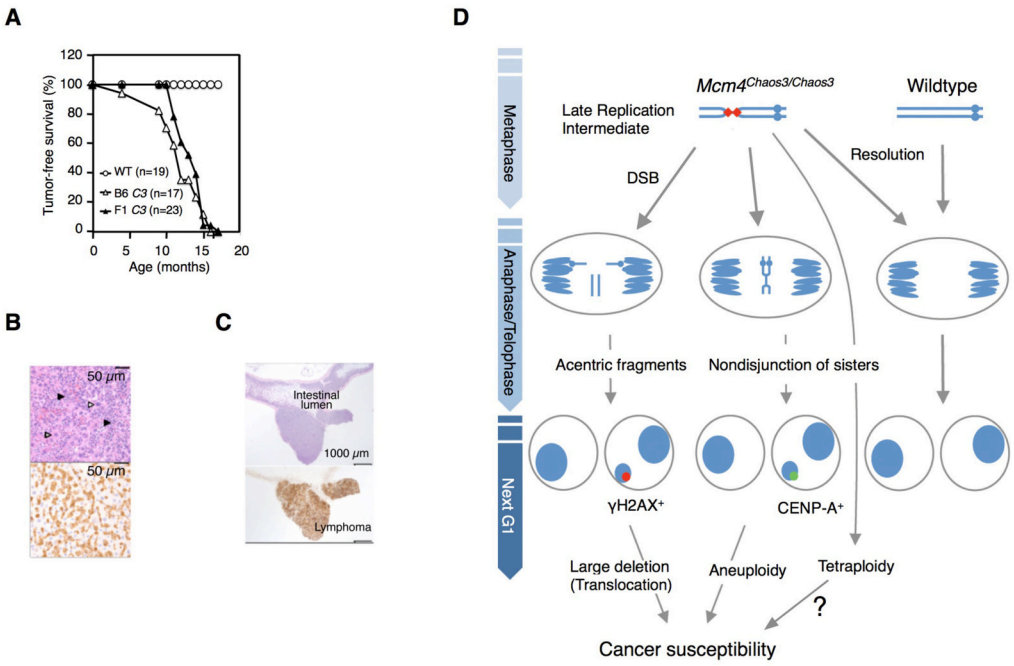

Figure 6. Many different types of spontaneous tumors are observed in *Mcm4*$^{Chaos3/Chaos3}$ mice

(A) Tumor-free survival curves for B6 and F1 *Mcm4*$^{Chaos3/Chaos3}$ (*C3*) and wildtype (WT) females.

(B) Representative images of histiocytic sarcomas. A hematoxylin and eosin (H&E) stain (top) shows a diffusely hypercellular liver area with round cells (black arrowheads) smaller than hepatocytes (unfilled arrowheads). Immunohistochemistry (IHC) with Mac-2, a macrophage marker, identified these small round cells (stained brown) as histiocytes (bottom).

(C) Representative images of F1 *Mcm4*^{Chaos3} gastrointestinal lymphomas, including an H&E image (top) and an IHC image with B220, a B-cell marker (bottom).

(D) A model for chromosome instability driven by a loss of dormant origins. A lack of dormant origins increases the frequency of unresolved replication intermediates marked with FANCD2 sister foci (red diamonds) in M phase. Although such lesions can be rescued in a Fanconi pathway-dependent manner, a significant fraction persists into anaphase, interconnecting sister chromatids. As a result, the disjunction of sisters is disrupted and lagging chromosomes occur. This has three possible consequences: 1) Tetraploidy may occur due to cytokinesis failure, when the frequency of nondisjunction is high (Shi and King, 2005), 2) Aneuploidy could occur due to the nondisjunction of a few sisters, forming MN positive for CENP-A, or 3) Breaks may arise when unresolved replication intermediates are converted into DSBs, generating acentric fragments. In this case, MN positive for γH2AX foci would be formed. These aberrations lead to multiple types of chromosome instability, thereby contributing to tumorigenesis.